ISSN: 2302-9285, DOI: 10.11591/eei.v13i4.7045

Enhancing voltage stability through wavelet-fuzzy control of hydrogen flow in OC-PEM fuel cell

Triyanto Pangaribowo^{1,2}, Wahyu Mulyo Utomo², Abdul Hamid Budiman³, Afarulrazi Abu Bakar², Deni Shidqi Khaerudini⁴

¹Department of Electrical Engineering, Faculty of Engineering, Universitas Mercu Buana, Jakarta, Indonesia ²Department of Electrical Engineering, Faculty of Electrical and Electronic Engineering, Universiti Tun Hussein Onn Malaysia, Malaysia

³Research Center for Energy Conversion and Conservation-National Research and Innovation Agency, South Tangerang, Indonesia

⁴Research Center for Advanced Materials, National Research and Innovation Agency, South Tangerang, Indonesia

Article Info

Article history:

Received Jun 22, 2023 Revised Feb 29, 2024 Accepted Mar 6, 2024

Keywords:

Fuzzy
Hydrogen flow
Open cathode proton exchange
membrane fuel cell
Voltage stability
Wavelet

ABSTRACT

Open cathode proton exchange membrane fuel cells (OC-PEM fuel cells) serve as electricity generators, utilizing hydrogen as an input source. While effective for fixed loads like residential applications, challenges arise in dealing with output voltage fluctuations caused by rapid load changes. These fluctuations not only impact fuel cell performance but also introduce instability in the supplied power. To solve this issue, the study proposes an innovative hydrogen flow control system employing a feedforward waveletfuzzy method. The primary goal of this control system is to enhance fuzzy control performance using wavelets, mitigating signal fluctuations and achieving optimal stability in fuel cell output voltage under constant load conditions. Wavelet functions act as filters on the fuzzy control input, minimizing fluctuations and refining the entire process. Additionally, a feedforward system is incorporated to maintain hydrogen flow at the set point value. The proposed control system is implemented on a validated model using experimental data. Performance analysis reveals that the proposed method effectively stabilizes voltage by accelerating the recovery time from disturbances.

This is an open access article under the CC BY-SA license.



2279

Corresponding Author:

Triyanto Pangaribowo

Department of Electrical Engineering, Faculty of Engineering, Universitas Mercu Buana

Jakarta Indonesia

Email: triyanto.pangaribowo@mercubuana.ac.id

1. INTRODUCTION

Open cathode proton exchange membrane (OC-PEM) fuel cells operate by necessitating a supply of oxygen and hydrogen gas as fuel to generate electrical energy through an electrochemical process [1]. In open cathode-type fuel cells, oxygen is introduced to the cathode via fans, and hydrogen gas is sourced from a pressurized tube [2]. This electrochemical reaction results in electricity production, with the sole byproducts being water and heat, establishing OC-PEM fuel cells as environmentally friendly [3]. OC-PEM fuel cells are versatile, suitable for both fixed and variable loads [4], [5]. In fixed load scenarios, they can efficiently power residential homes or offices, where stable operation is essential to meet consistent power demand [6]. In reality, achieving perfectly smooth output voltage of OC-PEM fuel cell is unattainable, leading to unavoidable undershoot voltage during loading [7]. Undershoot stress stems from insufficient reactants in the catalyst layer, typically observed under loading conditions [8]. When gas diffusion into the catalyst layer lags behind gas consumption through reactions, the reactant concentration becomes unstable,

Journal homepage: http://beei.org

2280 □ ISSN: 2302-9285

resulting in fluctuations in output performance [7]. These fluctuations, in turn, disrupt output stability, posing a threat to the reliability and safety of the fuel cell [9]. Severe undershoot behavior can even lead to reverse voltage and contribute to permanent degradation of the fuel cell [10]. Regulating a stable flow of hydrogen gas is one method used to increase the stability of the fuel cell output voltage [11]. Controlling hydrogen flow is critical in maintaining optimal operating conditions and reducing problems such as fluctuations, undershoot and overshoot in fuel cell output voltage [12]. A steady, well-controlled flow of hydrogen helps ensure a consistent supply of reactants to the fuel cell, minimizing variations in electrochemical reactions and contributing to a more stable output voltage [13].

Various control methods, including proportional-integral-derivative (PID) control [14] and fuzzy-PID [15] have been suggested for regulating hydrogen flow in fuel cells. However, the PID control system exhibits limitations in response time and accuracy when applied to highly dynamic non-linear systems [16]. Fuzzy control, while offering potential advantages, necessitates a thorough understanding to establish proper scaling, which can result in suboptimal performance of the control system [17]. Fuzzy control is employed to regulate the flow of hydrogen [18], relying on linguistic rules and fuzzy sets. The inherent ambiguity and subjectivity of linguistic rules can lead to a diminished level of control accuracy in specific situations [19]. Fuzzy controllers frequently encounter challenges in adjusting to unanticipated changes in system dynamics during the rule design phase [20]. Such limitations can impact the controller's effectiveness in managing unforeseen or swiftly changing conditions.

Hence, this paper introduces a novel hybrid control technique aimed at ensuring hydrogen flow stability and achieving voltage stability through the utilization of a wavelet-fuzzy controller. The wavelet component is employed to enhance the performance of fuzzy control by minimizing oscillations in the control input signal. This wavelet, comprising low-pass and high-pass filters, facilitates a rapid process without imposing computational burdens on the control system. The paper is structured into several sections, commencing with an introduction, followed by a method section encompassing the experimental setup, simulation model, and wavelet-fuzzy controller. Subsequently, the results and discussion section critically evaluates the findings. Finally, the conclusions section succinctly summarizes the key insights obtained.

2. METHOD

This section introduces the experimental setup, the simulation model for the OC-PEM fuel cell, and the schematic diagram of the control system. The simulation model was developed using MATLAB Simulink, incorporating mathematical equations pertinent to fuel cells.

2.1. Experimental setup of OC-PEM fuel cell

The fuel cell's performance underwent testing with a hydrogen flow input ranging from 1 to 8 L/min, utilizing an OC-PEM fuel cell with a maximum power capacity of 2.5~kW. Further elaboration on the experiment's parameters is provided in Table 1.

Aperiment parameter	s for the OC I L		
Parameters	Value		
Number of cells	73 cells		
Active area	5.5 cmx29 cm		
Thickness	4 mm		
Max power	2.5 kW		
Temperature	$31^{0}\text{C}-65^{0}\text{C}$		
Reactants	hydrogen and air		
Hydrogen flow rate	1-8 L/min		
Cooling	Air (cooling fan)		
Fan voltage	48 volt		
Purge duration/period	0.5 s/10 s		
Oxygen supply	Open cathode		

Table 1. Experiment parameters for the OC-PEM fuel cell

Although the OC-PEM fuel cell can produce up to 2.5 kW of power, this experiment is constrained by device limitations, utilizing a maximum power of 255 W. Hydrogen, supplied to the anode, and oxygen from the air, supplied to the cathode, are crucial for the fuel cell operation. The hydrogen gas supply system incorporates cylinders, regulators, and valves for precise control and delivery. As OC-PEM fuel cells generate heat during electrochemical reactions, a cooling system with three fans maintains optimal operating temperatures. An electrical load, ranging from 1 A to 10 A, is connected to the fuel cell stack to simulate practical power requirements. Various instruments monitor parameters such as voltage, current, temperature, and gas flow rate, providing essential data for performance analysis. Data acquisition systems collect, record,

П

and process information from these instruments, aiding in the comprehensive understanding of fuel cell behavior under diverse conditions. This experimental setup facilitates the exploration of PEM fuel cell efficiency, durability, and dynamic response, thereby making a substantial contribution to the optimization of fuel cells in this project. For further details, Figure 1 illustrates the components employed in the experiment.

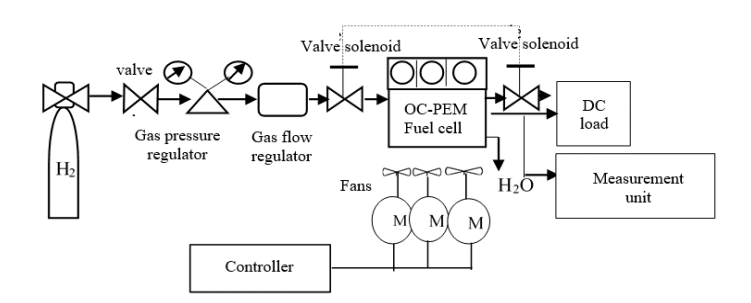


Figure 1. Schematic diagram of the OC-PEM fuel cell

The voltage drop pattern resulting from loading was derived from PEM fuel cell experiments. This pattern is represented by a polynomial as (1):

$$V_L = -((y^2) * 0.3467) + (49.716 * y) - (1724.3)$$
(1)

Here, V_L represents the voltage drop, and y denotes the voltage at open circuit voltage. The voltage drop pattern is experimentally obtained by systematically varying the electrical load applied to the fuel cell and measuring the resulting changes in voltage.

2.2. Simulation model of OC-PEM fuel cell

The simulation model for the OC-PEM fuel cell was constructed using MATLAB Simulink, employing mathematical equations as its foundation. The OC-PEM fuel cell simulation model is designed to predict key performance metrics, including voltage, current, and power output. The model aids in pinpointing optimal conditions conducive to achieving maximum power output and efficiency. The output of the fuel cell is typically represented as voltage, as indicated by (2) [21]:

$$V_{FC} = N_{cell}(E_{Nernst} - V_{Act} - V_{Ohmic} - V_{con})$$
 (2)

In the context where V_{FC} denotes the output voltage of the fuel cell, E_{Nernst} is the symbol employed to depict the thermodynamic potential and reversible voltage of the fuel cell [22], which equivalently represents its output voltage. Nevertheless, the actual output voltage is diminished owing to diverse voltage losses. These losses encompass activation losses at the anode and cathode (V_{Act}) , internal resistance losses (V_{Ohmic}) , and losses arising from the mass transfer of the reacting gas (V_{con}) [23]. The calculation for the Nernst voltage (E_{Nernst}) can be expressed using as (3):

$$E_{Nernst} = E^0 + \frac{RT}{2F} \left[\ln(P_{h_2}) + 0.5 \ln(P_{o_2}) \right]$$
 (3)

Here, E^0 symbolizes the reference potential, R stands for the universal gas constant, T represents the fuel cell operating temperature, and F denotes the Faraday constant. The voltage drop (V_{act}) arising from the activation of the anode and cathode [24] can be calculated using as (4):

$$V_{act} = -\left(\frac{R*T}{2*\alpha*F}\right) * \log\left(\frac{i_L}{i_0}\right) \tag{4}$$

The ohmic voltage drop (V_{ohmic}) is associated with the internal electronic resistance within the system and is computed using as (5):

$$V_{ohmic} = -(i_o * r) \tag{5}$$

The voltage drop caused by mass transportation effects, which influence the concentration of the reacting gases, is denoted as V_{con} [25]. It can be described using as (6):

$$V_{con} = -\alpha * i^k * \ln\left(1 - \frac{i_o}{i_l}\right) \tag{6}$$

2282 ISSN: 2302-9285

Static parameters in the OC-PEM fuel cell model are constants or factors that remain relatively stable under steady-state operating conditions. Table 2 displays the static model parameters utilized in this study.

Table 2. Parameters for the static model of OC-PEM fuel cell

Parameter	Value		
Number of cells (N _{cell})	73		
Max power	2.5 kW		
Operating temperature (T)	333 K		
Reference potential (E^0)	1.229 V		
Universal gas constant (R)	8.314 J/mol		
Faraday constant (F)	96485 C/mol		
Transfer coefficient (α)	0.5		
Limiting current density (i _L)	1.4 A/cm ²		
exchange current density (i ₀)	10^-6.912 A/cm ²		
Internal resistance (r)	0.19 Ohm.cm ²		

The mathematical equations for dynamic systems start by determining the molar constant value of the hydrogen valve (K_{H_2}) [26].

$$K_{H_2} = \frac{qH_2}{PH_2} = \frac{k_{an}}{\sqrt{MH_2}} \tag{7}$$

The symbol qH_2 represents the molar flow of hydrogen, while PH_2 signifies the partial pressure of hydrogen. Furthermore, MH_2 is the molar mass of hydrogen, and k_{an} is the anode valve constant. The mathematical equation for the partial pressure of hydrogen gas, represented by the symbol P_{H_2} [27], is as (8):

$$P_{H_2} = \frac{\frac{1}{K_{H_2}}}{1 + \tau H_2 s} \left(q_{H_2}^{in} - 2K_r I \right) \tag{8}$$

Where the modeling constant is indicated by K_r . The symbol $q_{H_2}^{in}$ represents the flow rate of hydrogen input, while the symbol $\tau H_2 s$ represents the hydrogen time constant. The stack current is denoted by the symbol I. To calculate τ_{H_2} use (9):

$$\tau_{H_2} = \frac{v_{an}}{\kappa_{H_2} RT} \tag{9}$$

In (10) can be employed to calculate the reacting hydrogen flow, denoted by the symbol $q_{H_2}^r$.

$$q_{H_2}^r = \frac{N_{cell}I}{2F} = 2K_r \tag{10}$$

The partial pressure of oxygen gas (P_{0_2}) at the fuel cell cathode can be calculated by (11):

$$P_{O_2} = \frac{{}^{1}\!/{}_{K_{O_2}}}{{}^{1+\tau_{O_2}}} \left(q_{O_2}^{in} - K_r I \right) \tag{11}$$

The molar flow of hydrogen gas (q_{H_2}) can be determined by (12):

$$q_{H_2} = \frac{N_{cell}I_{stack}}{2FU} \tag{12}$$

Here, the utilization factor, denoted by U with a value of 0.8, is employed. The stack voltage is calculated by multiplying the number of cells by the output voltage per cell, as indicated in (13):

$$V_{stack} = V_{cell} N_{cell} \tag{13}$$

Dynamic models assume a pivotal role in analyzing the overall performance and response time of fuel cell systems. Additional information about the parameters utilized in the dynamic model of the OC-PEM fuel cell is provided in Table 3. Dynamic models depict the rate at which a fuel cell system adjusts to alterations in input conditions. Figure 2 illustrates the dynamic model depicting the flow of hydrogen and oxygen.

Table 3. Parameters for the dynamic model of OC-PEM fuel cell

Parameter	Value		
Hydrogen time constants (τH_2)	3.37 s		
Oxygen time constants (τO_2)	6.74 s		
Hydrogen valves constants (KH_2)	0.843 mol/s.atm		
modeling constant (K_r)	1.4251×10 ⁻⁶ kmol s ⁻¹ atm		
Oxygen valves constants (KO_2)	2.52 mol/s.atm		

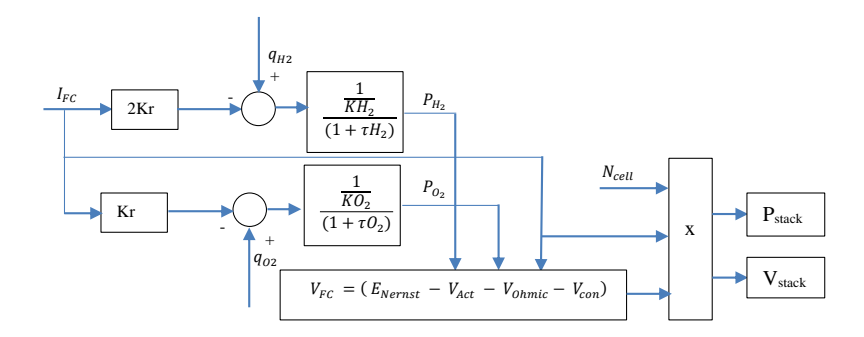


Figure 2. Dynamic model of OC-PEM fuel cell

2.3. Wavelet-fuzzy controller

This study integrates wavelet transform into a hybrid control system alongside a fuzzy controller. Within this framework, wavelets serve as a filtering technique for input signals directed to the fuzzy controller. The established OC-PEM fuel cell model is employed to realize a wavelet-fuzzy control system, and Figure 3 illustrates the block diagram of this integrated system.

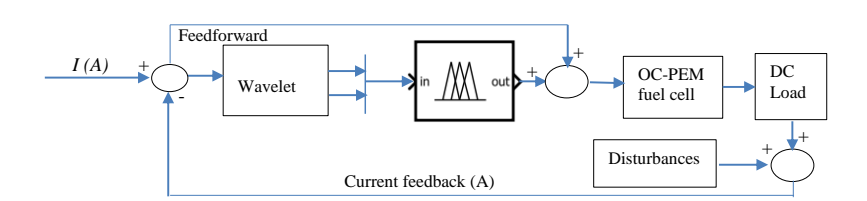


Figure 3. Structure of wavelet-fuzzy controller

2.3.1. Wavelet transforms

In this study, we employ the biorthogonal cohen-daubechies-feauveau (CDF) 5/3 wavelet transformation due to its benefits, including a lack of overshoot and fast response [28]. The CDF 5/3 wavelet utilizes two sets of filter coefficients, distinguishing between those used in the analysis (decomposition) stage and those employed in the synthesis (reconstruction) stage. Specifically, for the analysis stage of the CDF 5/3 wavelet, the filter coefficients are as (14) and (15):

$$h(z) = -\frac{1}{8}z^{-2} + \frac{1}{4}z^{-1} + \frac{3}{4} + \frac{1}{4}z^{1} - \frac{1}{8}z^{2}$$
(14)

$$g(z) = -\frac{1}{2}z^{-1} + 1 - \frac{1}{2}z^{1} \tag{15}$$

Additionally, the synthesis (reconstruction) filter coefficients are intricately linked to the analysis filter coefficients, guided by specific properties to guarantee a flawless reconstruction process [29]. Specifically, the synthesis filter coefficient for CDF 5/3 is (16) and (17):

$$\bar{h}(z) = \frac{1}{2}z^{-1} + 1 + \frac{1}{2}z^{1} \tag{16}$$

$$\bar{g}(z) = -\frac{1}{8}z^{-2} - \frac{1}{4}z^{-1} + \frac{3}{4} - \frac{1}{4}z^{1} - \frac{1}{8}z^{2}$$
(17)

2284 □ ISSN: 2302-9285

In Figure 4, the CDF 5/3 wavelet structure is depicted, wherein the production coefficient, denoted by α , is represented as -1/2, and the update coefficient, symbolized by β , possesses a value of β =-1/4. According to the information in Figure 4, there are two inputs for the wavelet: the error (e(k)) and the rate of change of the error, denoted as ec(k).

$$e(k) = I_{fc}^* - I_{fc} (18)$$

$$ec(k) = e(k) - e(k-1)$$
 (19)

Where I_{fc}^* is the fuel cell set point current.

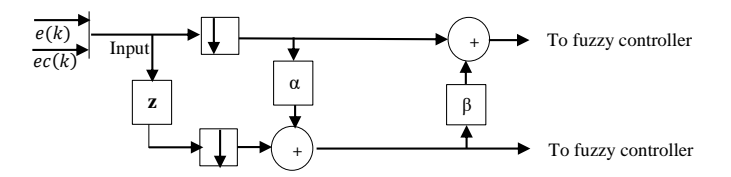


Figure 4. Structure of CDF 5/3 wavelet

2.3.2. Fuzzy controller

The suggested fuzzy logic controller manages the hydrogen flow by adjusting the current by (12). In Figure 5, a fuzzy control structure is illustrated, featuring two inputs derived from the CDF 5/3 wavelet output, specifically the approximation and details.

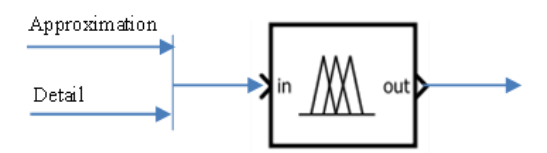


Figure 5. Structure of fuzzy controller

Gaussian-type membership functions are employed for the error (e), error change (ec), and control output (u_{H_2}) . The fuzzy domains for e and ec are defined within the range of [-0.5, 0.5], whereas for u_{H_2} , the range is [-0.2, 0.2]. The fuzzy set for e, ec, and u_{H_2} comprises Ng_Bg representing negative big, Ng_Sm for negative small, Zo for zero, Po_Sm for positive small, and Po_Bg indicating positive big. The fuzzy control rule base is detailed in Table 4. Here are some examples of fuzzy rule bases:

If e is Ng_B_g and ec is $N_g_B_g$ then u_{H_2} is Ze If e is Z_e and ec is $N_g_B_g$ then u_{H_2} is $N_g_B_g$ If e is Z_e and ec is $N_g_S_m$ then u_{H_2} is $N_g_S_m$

Table 4. Rule base of fuzzy control						
Α.	Ec					
e	Ng_Bg	Ng_Sm	Ze	Po_Sm	Po_Bg	
Ng_Bg	Ze	Ze	Ng_Bg	Ze	Ze	
Ng_Sm	Ze	Ze	Ng_Sm	Ze	Ze	
Ze	Ng_Bg	Ng_Sm	Ze	Po_Sm	Po_Bg	
Po_Sm	Ze	Ze	Po_Sm	Ze	Ze	
Po Ro	70	70	Po Ro	70	70	

The centroid defuzzification method calculates the output value based on the center of gravity of the output membership function, as expressed by (20):

$$u_{H_2} = \frac{\sum_{i=0}^{n} \mu_{Ci}(u_{H_{2i}})u_{H_{2i}}}{\sum_{i=0}^{n} \mu_{Ci}(u_{H_{2i}})}$$
 (20)

The fuzzy logic controller employs gaussian membership functions to represent the degree of membership for both input and output variables. Figure 6 illustrates the input variables for error (e) and error change (ec). Meanwhile, for the control output variable, it is indicated in Figure 7.

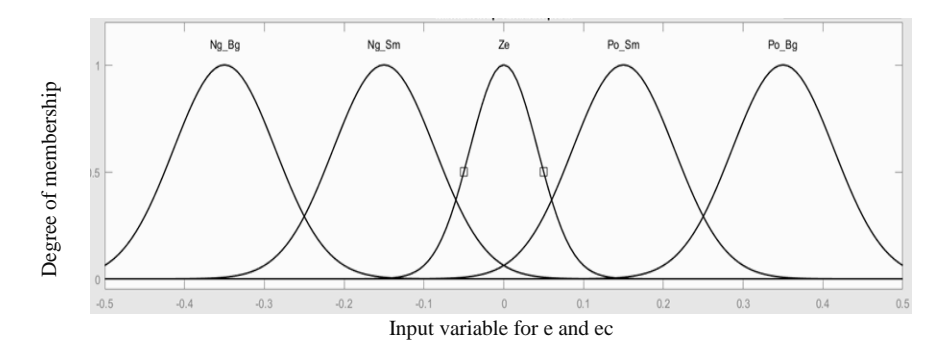


Figure 6. Gaussian membership function of the error (e) and error change (ec)

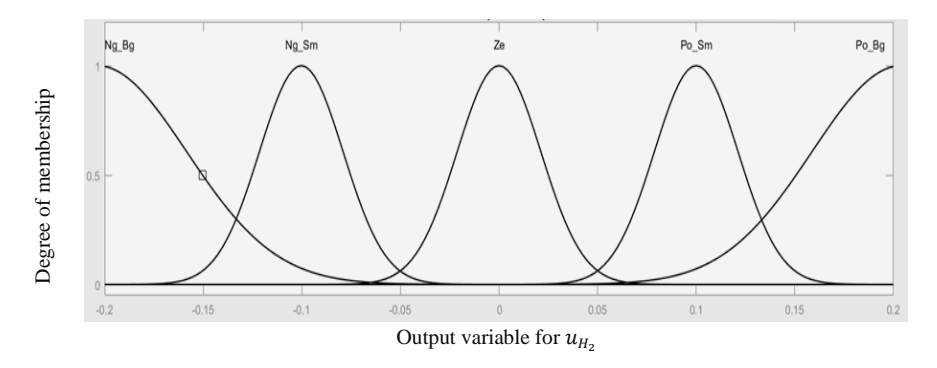


Figure 7. Gaussian membership function of control output (u_{H_2})

3. RESULTS AND DISCUSSION

3.1. Discoveries from simulation and experimental results

The model validation involved a comparison between experimental and simulation results, as depicted in Figure 8. Figure 8 illustrates the relationship between current and power obtained with a constant hydrogen flow input of 8 L/min. During this investigation, the current load was incrementally raised from 1 A until it reached a maximum of 7.87 A, and the power began to decline after reaching 252.4 W. The experimental results indicated that at low loads, ranging from 1 to 6 A, there were no significant output voltage fluctuations. However, as depicted in Figure 9, fluctuations become noticeable with an increase in the load. This image also highlights the presence of undershoot voltage, signifying that the output does not reach the maximum voltage.

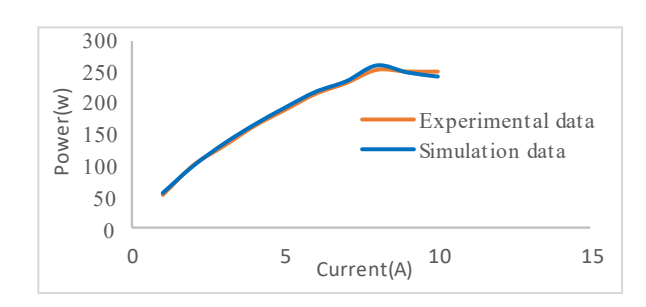


Figure 8. Maximum load for hydrogen input 8 L/min

Instabilities in the output voltage lead to variations in the current and power supplied to the load, as evident in Figure 10. Additionally, Figure 10 reveals fluctuations in the load current at 7.5 A, yet the current does not reach the targeted set point value.

2286 □ ISSN: 2302-9285

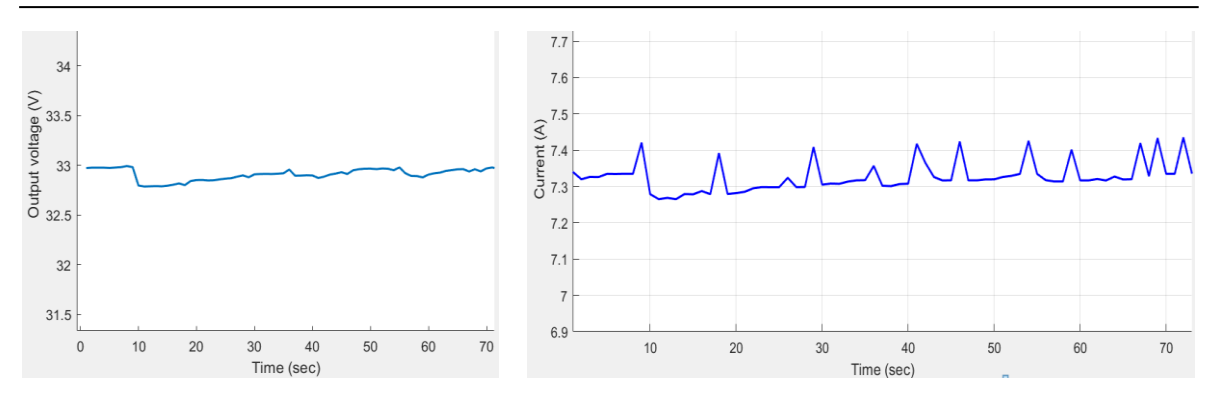
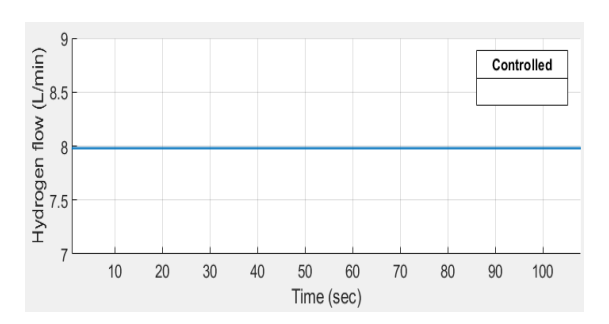


Figure 9. Output voltage under a 7.5 A load

Figure 10. Output current fluctuation

3.2. Wavelet-fuzzy controller performance

Evaluating the performance of the wavelet-fuzzy controller involves utilizing an 8 L/min hydrogen flow input. Figure 11 exhibits a well-regulated and stable flow of hydrogen gas. In testing the control system, a set point value of 7.5 A is applied, considering fluctuating current disturbances, as illustrated in Figure 10. The outcomes of voltage response testing with wavelet-fuzzy control are depicted in Figure 12.



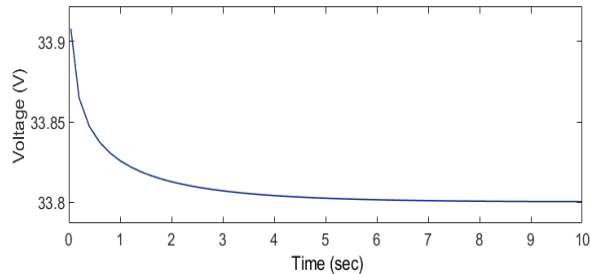


Figure 11. Hydrogen flow output of the wavelet-fuzzy control system

Figure 12. Output voltage response of the wavelet-fuzzy control system

Figure 12 demonstrates the exceptional stability of the output voltage, maintaining a constant value of $33.8\,$ V. This indicates the effective suppression of fluctuations through the proposed system control strategy. Comparing the accuracy of the output voltage with the optimal value of $34\,$ V yields a high accuracy of approximately 99.412%.

4. CONCLUSION

This paper introduces a hydrogen flow control system aimed at ensuring voltage stability using wavelet-fuzzy. The application of this control system is demonstrated under fixed loads. Experimental findings reveal fluctuations in the output voltage when a load of 7.5 A is applied, characterized by undershoot within a range of 0.1 V to 0.3 V below the set point value. Upon implementing the proposed control system, a hydrogen flow stability of 8 L/min is achieved, contributing to the stability of the output voltage at 33.8 V, closely approaching the target value of 34 V. The performance analysis of the control system indicates high accuracy, reaching 99.4%.

ACKNOWLEDGEMENTS

The author acknowledges the financial support received from Universitas Mercu Buana, Jakarta, Indonesia, and extends appreciation to the National Research and Innovation Agency of the Republic of Indonesia (BRIN) and Universiti Tun Hussein Onn Malaysia (UTHM) for their significant scientific and substantial support.

П

REFERENCES

- [1] S. A. Atyabi, E. Afshari, and N. Shakarami, "Three-dimensional multiphase modeling of the performance of an open-cathode PEM fuel cell with additional cooling channels," *Energy*, vol. 263, p. 125507, Jan. 2023, doi: 10.1016/j.energy.2022.125507.
- [2] Y. Yang *et al.*, "Overall and local effects of operating parameters on water management and performance of open-cathode PEM fuel cells," *Applied Energy*, vol. 315, p. 118978, Jun. 2022, doi: 10.1016/j.apenergy.2022.118978.
- [3] D. Huo, Q. Peng, and C. M. Hall, "Koopman-Based Modeling of an Open Cathode Proton Exchange Membrane Fuel Cell Stack," IFAC-PapersOnLine, vol. 56, no. 3, pp. 67–72, 2023, doi: 10.1016/j.ifacol.2023.12.002.
- [4] C. Zhao, B. Li, L. Zhang, Y. Han, and X. Wu, "Novel optimal structure design and testing of air-cooled open-cathode proton exchange membrane fuel cell," *Renewable Energy*, vol. 215, p. 118899, Oct. 2023, doi: 10.1016/j.renene.2023.06.020.
- [5] H. Mehida, A. Aboubou, and M. Y. Ayad, "Reliability improvement of multi-phase interleaved DC-DC converters for fuel cell electric vehicle applications," *Bulletin of Electrical Engineering and Informatics*, vol. 12, no. 5, pp. 2553–2560, Oct. 2023, doi: 10.11591/eei.v12i5.4674.
- [6] M. Fattahi, "Fuzzy sliding mode control of hydrogen flow in PEM fuel cell system for residential power generation," in 2017 5th International Conference on Control, Instrumentation, and Automation (ICCIA), pp. 1–6, Nov. 2018, doi: 10.1109/icciautom.2017.8373943.
- [7] W. Chen, B. Chen, K. Meng, H. Zhou, and Z. Tu, "Experimental study on dynamic response characteristics and performance degradation mechanism of hydrogen-oxygen PEMFC during loading," *International Journal of Hydrogen Energy*, vol. 48, no. 12, pp. 4800–4811, Feb. 2023, doi: 10.1016/j.ijhydene.2022.11.036.
- [8] Q. Yang, B. Gao, G. Xiao, and D. Jin, "Analysis of PEMFC undershoot behavior and performance stabilization under transient loading," *International Journal of Hydrogen Energy*, vol. 50, pp. 1358–1372, Jan. 2024, doi: 10.1016/j.ijhydene.2023.07.013.
- [9] M. Zadehbagheri, M. J. Kiani, and T. Sutikno, "Investigation of the Effects of Fuel Cells on V-Q & V-P Characteristics," *Journal of Robotics and Control (JRC)*, vol. 3, no. 4, pp. 535–545, Jul. 2022, doi: 10.18196/jrc.v3i4.14855.
- [10] R. Pan, D. Yang, Y. Wang, and Z. Chen, "Health degradation assessment of proton exchange membrane fuel cell based on an analytical equivalent circuit model," *Energy*, vol. 207, p. 118185, Sep. 2020, doi: 10.1016/j.energy.2020.118185.
- [11] Z. Yu, F. Liu, and C. Li, "Numerical study on effects of hydrogen ejector on PEMFC performances," *Energy*, vol. 285, p. 129481, Dec. 2023, doi: 10.1016/j.energy.2023.129481.
- [12] Z. R. Guo, H. Chen, H. Guo, and F. Ye, "Dynamic response and stability performance of a proton exchange membrane fuel cell with orientational flow channels: An experimental investigation," *Energy Conversion and Management*, vol. 274, p. 116467, Dec. 2022, doi: 10.1016/j.enconman.2022.116467.
- [13] X. Bai, L. Luo, B. Huang, Q. Jian, and Z. Cheng, "Performance improvement of proton exchange membrane fuel cell stack by dual-path hydrogen supply," *Energy*, vol. 246, p. 123297, May 2022, doi: 10.1016/j.energy.2022.123297.
- [14] F. R. Maulana, K. Indriawati, and R. A. Wahyuono, "Reactant Control Strategies for Maximizing Efficiency in Open Cathode PEM Fuel Cell," in 2023 8th International Conference on Instrumentation, Control, and Automation (ICA), Aug. 2023, pp. 30–35, doi: 10.1109/ICA58538.2023.10273067.
- [15] W. Wang, J. Chen, C. Xiao, and N. Cheng, "Adaptive fuzzy control method of hydrogen fuel cell gas supply system," *Journal of Physics: Conference Series*, vol. 1983, no. 1, p. 012051, Jul. 2021, doi: 10.1088/1742-6596/1983/1/012051.
- [16] Y. Huang and Y. Huang, "Research on PID Parameter Self-Tuning Speed Control System Based on Grasshopper Optimazation Algorithm-Optimized BP Neural Network," in 2023 3rd International Conference on Energy, Power and Electrical Engineering, EPEE 2023, Sep. 2023, pp. 1444–1450, doi: 10.1109/EPEE59859.2023.10351813.
- [17] F. Behrooz, N. Mariun, M. H. Marhaban, M. A. M. Radzi, and A. R. Ramli, "Review of control techniques for HVAC systems-nonlinearity approaches based on fuzzy cognitive maps," *Energies*, vol. 11, no. 3, p. 495, Feb. 2018, doi: 10.3390/en11030495.
- [18] M. Fattahi, "Fuzzy sliding mode control of hydrogen flow in PEM fuel cell system for residential power generation," 2017 5th International Conference on Control, Instrumentation, and Automation (ICCIA), Shiraz, Iran, 2017, pp. 1-6, doi: 10.1109/ICCIAutom.2017.8373943.
- [19] Z. Ai, Z. Xu, and X. Shu, "Limit Theory and Differential Calculus of Intuitionistic Fuzzy Functions with Several Variables," IEEE Transactions on Fuzzy Systems, vol. 28, no. 12, pp. 3367–3375, Dec. 2020, doi: 10.1109/TFUZZ.2019.2950881.
- [20] S. Budiyanto, L. M. Silalahi, F. A. Silaban, U. Darusalam, S. Andryana, and I. M. F. Rahayu, "Optimization of Sugeno Fuzzy Logic Based on Wireless Sensor Network in Forest Fire Monitoring System," in *Proceeding - 2020 2nd International Conference* on Industrial Electrical and Electronics, ICIEE 2020, pp. 126–134, Oct. 2020, doi: 10.1109/ICIEE49813.2020.9277365.
- [21] N. Rifai, J. Sabor, C. Alaoui, R. Petrone, and H. Gualous, "Dynamic modeling of an open cathode PEM fuel cell for automotive energy management applications," *International Journal of Power Electronics and Drive Systems*, vol. 13, no. 3, pp. 1406–1418, Sep. 2022, doi: 10.11591/ijpeds.v13.i3.pp1406-1418.
- [22] F. Chen, L. Zhang, and J. Jiao, "Modelling of humidity dynamics for open-cathode proton exchange membrane fuel cell," *World Electric Vehicle Journal*, vol. 12, no. 3, p. 106, Aug. 2021, doi: 10.3390/wevj12030106.
- [23] X. Bai and Q. Jian, "Decoupling strategy for react-air supply and cooling of open-cathode proton exchange membrane fuel cell stack considering real-time membrane resistance estimation," *Journal of Cleaner Production*, vol. 410, p. 137288, Jul. 2023, doi: 10.1016/j.jclepro.2023.137288.
- [24] B. O. Emmanuel, P. Barendse, and J. Chamier, "Effect of Anode Stoichiometry and Back Pressure on the Performance of PEMFCs," in 2018 IEEE PES/IAS PowerAfrica, PowerAfrica 2018, Jun. 2018, pp. 1–6, doi: 10.1109/PowerAfrica.2018.8521183.
- [25] B. Li, Z. Guo, L. Zeng, J. Fu, C. Sheng, and X. Li, "Optimization of Parameter Matching for PEM Fuel Cell Hybrid Power System," in *Chinese Control Conference, CCC*, Jul. 2023, vol. pp. 6340–6345, 2023, doi: 10.23919/CCC58697.2023.10240722.
- [26] U. K. Chakraborty, "A new model for constant fuel utilization and constant fuel flow in fuel cells," *Applied Sciences* (Switzerland), vol. 9, no. 6, p. 1066, Mar. 2019, doi: 10.3390/app9061066.
- [27] K. Mammar, F. Saadaoui, and A. Hazzab, "Development and simulation of a PEM fuel cell model for prediction of water content and power generation," vol. 4, no. 2017, pp. 289–299, 2018, doi: 10.22104/ijhfc.2018.2792.1168.
- [28] M. Sushmitha, S. Chetan, and S. Sarkar, "An Efficient High-Speed Lifting Based 1D/2D-DWT VLSI Architecture Using CDF-5/3 Wavelet Transform for Image Processing Applications," in Proceedings 5th IEEE International Conference on Recent Trends in Electronics, Information and Communication Technology, RTEICT 2020, pp. 269–274, Nov. 2020, doi: 10.1109/RTEICT49044.2020.9315649.
- [29] S. Krishna, D. Kumar, and V. K. Dwivedi, "Biorthogonal Wavelets for Multiresolution Image Compression," in 2022 2nd International Conference on Power Electronics and IoT Applications in Renewable Energy and its Control, PARC 2022, pp. 1–7, Jan. 2022, doi: 10.1109/PARC52418.2022.9726558.

BIOGRAPHIES OF AUTHORS





Wahyu Mulyo Utomo was born in Pati, Indonesia, in 1969. He received B.S. degree in Electrical Engineering from Universitas Brawijaya Malang, in 1993, M.S. degree in Electrical Engineering from the Institute Sepuluh Nopember Surabaya, in 2000, and Dr. Eng Degree from Universiti Teknologi Malaysia in 2007. He is currently an Associate Professor at the Department of Electrical Power Engineering, Faculty of Electrical and Electronic Engineering, Universiti Tun Hussein Onn Malaysia. His current research interests include the area of power electronics and motor drives control. He can be contacted at email: wahyu@uthm.edu.my.



Abdul Hamid Budiman is a researcher at the Research Center for Energy Conversion and Conservation, National Research and Innovation Agency of The Republic of Indonesia (BRIN) with a focus on fuel cell and hydrogen technology. He completed his Doctoral Degree in Chemical Engineering from the University of Indonesia (2011). He is a member and a treasure of Indonesia Fuel Cell and Hydrogen Energy (IFHE). He can be contacted at email: abdu031@brin.go.id.



Afarulrazi Abu Bakar received his B.Eng. degree in Electrical Engineering from Universiti Teknologi Mara (UiTM), Malaysia, in 2004 and M.Eng. and Ph.D., degrees from Universiti Tun Hussein Onn Malaysia (UTHM), in 2019 and 2007, respectively. He has been working as a Senior Lecturer at the Department of Electrical Power Engineering, Faculty of Electrical and Electronic Engineering, UTHM, since 2007. His current research interests include renewable energy application, DC/DC converters, multiple-input converters, multiphase converters, resonant converters, and advanced controller design. He can be contacted at email: afarul@uthm.edu.my.



Deni Shidqi Khaerudini Deli si sa Research Professor (Professor) at Research Center for Advanced Materials, National Research and Innovation Agency (BRIN), Indonesia. He also as a faculty member at the Department of Mechanical Engineering, Universitas Mercu Buana, since 2017 to present. He earned his Ph.D. (Dr. Eng.) in 2016 from the Hirosaki University, Japan for his research in the area of ceramics processing techniques for intermediate temperature solid oxide fuel cells (SOFC). He is also heading the Banten Chapter of the Indonesian Researcher Union (PPI) and as the Deputy II of Indonesia Fuel Cell and Hydrogen Energy (IFHE). He can be contacted at email: deni.shidqi.khaerudini@brin.go.id.